A Chimeric Elongation Factor Containing the Putative Guanine Nucleotide Binding Domain of Archaeal EF-1α and the M and C Domains of Eubacterial EF-Tu†

Paolo Arcari, Mariorosario Masullo, Alessandro Arcucci, Giuseppe Ianniciello, Barbara de Paola, and Vincenzo Bocchini*

Dipartimento di Biochimica e Biotecnologie Mediche, Università di Napoli Federico II, via S. Pansini, 5, I-80131 Napoli, Italy

Received February 22, 1999; Revised Manuscript Received May 28, 1999

ABSTRACT: A recombinant chimeric elongation factor containing the region of EF-1α from *Sulfolobus solfataricus* harboring the site for GDP and GTP binding and GTP hydrolysis (*Ss*G) and domains M and C of *Escherichia coli* EF-Tu (*Ec*MC) was studied. *Ss*G-*Ec*MC did not sustain poly(Phe) synthesis in either *S. solfataricus* or *E. coli* assay system. This was probably due to the inability of the chimera to interact with aa-tRNA. The three-dimensional modeling of *Ss*G-*Ec*MC indicated only small structural differences compared to the *Thermus aquaticus* EF-Tu in the ternary complex with aa-tRNA and GppNHp, which did not account for the observed inability to interact with aa-tRNA. The addition of the nucleotide exchange factor *Ss*EF-1*β* was not required for poly(Phe) synthesis since the chimera was already able to exchange [^{3}H]GDP for GTP at very high rate even at 0 °C. Compared to that of *Ss*EF-1α, the affinity of the chimera for guanine nucleotides was increased and the k_{cat} of the intrinsic GTPase was 2-fold higher. The heat stability of *Ss*G-*Ec*MC was 3 and 13 °C lower than that displayed by *Ss*G and *Ss*EF-1α, respectively, but 30 °C higher than that of *Ec*EF-Tu. This pattern remained almost the same if the melting curves of the proteins being investigated were considered instead. The chimeric elongation factor was more thermophilic than *Ss*G and *Ss*EF-1α up to 70 °C; at higher temperatures, inactivation occurred.

The primary structure of elongation factor 1α (EF-1α)[1] and EF-Tu has been determined in many organisms (*1*). They all exhibit stretches of identical sequence mainly at the N-terminal region which contains the guanine nucleotide binding motifs (*2*). X-ray diffraction studies with *Escherichia coli* EF-Tu·GDP (*3*, *4*) and *Thermus thermophilus* (*5*) and *Thermus aquaticus* EF-Tu·GTP (*6*) revealed that EF-Tu is made of three distinct structural domains, the nucleotide binding G domain, the middle M domain, and the C-terminal C domain. The substitution of GDP for GTP provokes a dramatic difference in the orientation of the G domain with respect to the M and C domains (*7*).

EF-1α from *Sulfolobus solfataricus* is a monomeric protein made of 435 amino acid residues (*8*); its three-dimensional (3D) structure is being investigated (*9*). It is highly thermostable (*10*), belongs to the family of the GTP-binding proteins (*11*), and exhibits an intrinsic GTPase activity stimulated by NaCl at molar concentrations (*12*). With the lack of structural data, the definition of the functional role of specific regions of *Ss*EF-1α has been attempted by measuring the biochemical properties of *Ss*G and *Ss*GM regions (*13*). *Ss*G contained the site for GDP and GTP binding and GTP hydrolysis, whereas the C and M regions were important for the regulation of the affinity of *Ss*G for GDP and GTP, the interaction with ribosome, and the thermostability of the intact *Ss*EF-1α (*13*).

To asses the role in a protein molecule of specific regions, another approach was the construction of chimeras engineered from homologous proteins (*14*−*16*). With this approach, *Ss*EF-1α and *Ec*EF-Tu are interesting models since although they are homologous enzymes, their GTPase activities differ in a number of properties such as the mechanism of the catalytic reaction, the different affinity toward effectors, antibiotics, and ligands, and the different behaviors with respect to physical and chemical denaturants (*11*, *12*). Therefore, the construction of a chimeric elongation factor made of the thermophilic archaeal *Ss*G and the mesophilic eubacterial domain *Ec*MC was intriguing since it allowed us to investigate the effects on the functional properties produced by the interaction between complementary domains of proteins isolated from organisms living under very different environmental conditions. The stability of the chimera was evaluated by measuring its heat inactivation and denaturation following exposure to heat.

† This investigation was supported by Ministero dell'Università e della Ricerca Scientifica e Tecnologica (PRIN 1997), Consiglio Nazionale delle Ricerche (Rome), and the European Community Human Capital and Mobility Programme (Contract ERBCHRXCT 940510).

* Corresponding author. Telephone: +39-081-7463120. Fax: +39-081-7463653. E-mail: bocchini@unina.it.

[1] Abbreviations: *Ec*, *Escherichia coli*; *Ss*, *Sulfolobus solfataricus*; *Ta*, *Thermus aquaticus*; EF, elongation factor; G, M, and C, structural domains of *Ec*EF-Tu and putative domains of *Ss*EF-1α; *Ss*G-*Ec*MC, chimeric elongation factor containing *Ss*G and domains M and C of *Ec*EF-Tu; *Ec*G-*Ss*MC, chimeric elongation factor containing domain G of *Ec*EF-Tu and the M and C domains of *Ss*EF-1α; GTPase^{Na}, intrinsic *Ss*EF-1α GTPase triggered by 3.6 M NaCl; IPTG, isopropyl *β*-D-thiogalactopyranoside; GST, gluthatione *S*-acetyltransferase; Gpp(NH)p, guanyl-5′-yl imidodiphosphate; K_{iGDP} and $K_{iGpp(NH)p}$, inhibition constants for GDP and Gpp(NH)p, respectively; *E*, Δ*S**, and Δ*G**, energy, entropy, and free energy of activation, respectively.

10.1021/bi990418d CCC: $18.00
Published on Web 09/03/1999

MATERIALS AND METHODS

Chemicals, Enzymes, and Buffers. Restriction enzymes, modifying enzymes, labeled compounds, and chemicals were as previously reported (*17*); plasmid DNA, genomic DNA, and labeled probes were prepared as described previously (*18*).

The following buffers were used: buffer A [50 mM Tris-HCl (pH 7.8), 50 mM KCl, 10 mM $MgCl_2$, 15% glycerol, and 1 mM phenylmethanesulfonyl fluoride], buffer B [20 mM Tris-HCl (pH 6.8), 10 mM $MgCl_2$, and 20% glycerol], buffer C [20 mM Tris-HCl (pH 7.8), 10 mM $MgCl_2$, and 50 mM KCl], and buffer D [20 mM Tris-HCl (pH 7.8), 10 mM $MgCl_2$, and 1 mM dithiothreitol].

Plasmid Construction and Expression and Purification of the Chimeric Elongation Factor. The pGEX-2T plasmid containing the *E. coli tuf*A gene (*19*) fused to the gene encoding GST (*20*) was used as template to synthesize a DNA fragment encoding the MC domain of *Ec*EF-Tu. The two primers were AGAGCGTGCGATTGGAATTCCGTT (EX5) corresponding to positions 609−632 of the *Ec*EF-Tu gene (as numbered from the start codon) and the reverse primer TTTCACCGTCATCACCGAAA (EX4) corresponding to the region of the pGEX-2T vector close to the polylinker. EX5 contained an *Eco*RI restriction site that corresponds to the sequence encoding amino acid residues Asp207 and Lys208, which in *Ec*EF-Tu separate domain G and domains M and C (*3*). A *Sma*I restriction site is also present in the *E. coli* DNA after the stop codon of the EF-Tu gene. The PCR product was then cleaved with the restriction enzymes *Eco*RI and *Sma*I, purified on agarose gel, cloned into a pT7-7 vector harboring the *Ss*EF-1α gene (*21*), and cleaved with the same restriction enzymes. The new vector contained an open reading frame encoding a 420-residue protein. The recombinant clone was then transferred into *E. coli* BL21(DE3) cells which express the T7 RNA polymerase under the control of the inducible lac UV5 promoter (*22*). The transformed cells were then used to inoculate 10 mL of Luria broth containing 100 μg/mL ampicillin and grown overnight at 37 °C. The culture was then diluted 1:100 in a final volume of 1 L and grown up to an absorbance of 0.7 at 600 nm. Induction was performed by adding isopropyl β-D-thiogalactopyranoside (IPTG) to a final concentration of 0.4 mM. After induction for 3 h, the bacterial cells were collected by centrifugation, resuspended in buffer A (6 mL/g of wet cells), and disrupted with a French press at 1000 psi followed by sonication (three 30 s impulses at 100 W). The chimeric elongation factor accumulated in the inclusion bodies from which it was purified according to the procedure hereafter described. The pellet of the S30 fraction was resuspended in 20 mL of 8 M urea and incubated overnight at 37 °C. The sample was centrifuged, and the supernatant was then dialyzed against buffer B and loaded onto a Mono Q (HR 10/10) column equilibrated with the same buffer and connected to an FPLC system (Pharmacia) operating at room temperature at a flow rate of 2 mL/min. The chimeric elongation factor was collected in the flow through. The active fractions were analyzed on SDS−PAGE, and only those exhibiting a single protein band were pooled together, dialyzed against buffer B containing 50% (v/v) glycerol, and stored at −20 °C.

Chimeric Elongation Factor Assays and Characterization. Poly(U)-directed poly(Phe) synthesis and the isolation of total tRNA and ribosome from *S. solfataricus* were performed at 60 °C as previously described (*10*). Poly(U)-directed protein synthesis tested with the *E. coli* components was performed as previously reported (*23*).

The preparation of Phe-$tRNA^{Phe}$, the formation of the ternary complex between the chimeric elongation factor, [γ-^{32}P]GTP and Phe-$tRNA^{Phe}$, and the protection of spontaneous deacylation of the Phe-$tRNA^{Phe}$ were carried out as previously reported (*23*).

The ability of the chimera to form a binary complex with [^{3}H]GDP was assayed as described previously (*10*). The number of [^{3}H]GDP binding sites and the equilibrium dissociation constant (K_d) of the complex of the chimera and [^{3}H]GDP were determined with Scatchard plots; values of K_d for GTP were obtained by competitive binding experiments in the presence of 25 μM [^{3}H]GDP at different GTP concentrations, and the dissociation rate constants for the *Ss*G-*Ec*MC·[^{3}H]GDP complex were determined as previously reported (*10*).

The $GTPase^{Na}$ activity of the chimera was measured in the presence of 3.6 M NaCl (*12*). Unless otherwise indicated, the reaction mixture contained 0.5−1.0 μM *Ss*G-*Ec*MC and 50 μM [γ-^{32}P]GTP (specific activity of 50−100 cpm/pmol) in 200 μL of buffer D. The reaction was followed kinetically, and at appropriate time intervals depending on the temperature, 40 μL aliquots were withdrawn and analyzed for the amount of $^{32}P_i$ that was released. k_{cat} of $GTPase^{Na}$, K_m of [γ-^{32}P]GTP, the inhibition constants for GDP and Gpp(NH)p, and the energetic parameters of activation were determined as previously reported (*12*, *13*).

The effect of kirromicyn on the intrinsic GTPase activity of *Ss*G-*Ec*MC, *Ss*EF-1α, and *Ss*G was tested as previously described (*24*) in the presence of 50 μM antibiotic.

The values of the kinetic parameters reported in this paper represent average values of three to six different determinations.

Measurement of the Thermophilicity and Heat Stability of SsG-EcMC. The thermophilicity of the chimera was evaluated by measuring the level of $GTPase^{Na}$ in the temperature range of 40−85 °C. At each temperature, the reaction was followed kinetically as described above. The effect of temperature on the [^{3}H]GDP−GDP and [^{3}H]GDP−GTP exchange reactions on the preformed *Ss*G-*Ec*MC·[^{3}H]-GDP complex was assessed as previously reported (*13*). The mixture contained the preformed labeled binary complex at a concentration of 0.6 μM (specific activity of about 10^3 cpm/pmol) in 120 μL of buffer C. The exchange reaction was started by adding 2 mM unlabeled GDP or GTP; at appropriate time intervals, 25 μL aliquots were withdrawn and the residual radioactive binary complex was identified by the nitrocellulose filter technique. The data were treated according to first-order kinetics and then analyzed by the Arrhenius equation. The energetic parameters of activation were calculated as previously reported (*25*). The effect of 0.1 μM *Ss*EF-1β on the [^{3}H]GDP−GTP exchange on the preformed *Ss*G-*Ec*MC·[^{3}H]GDP complexes was tested at 40 °C as described previously (*13*).

The heat inactivation of the chimeric elongation factor and other proteins was assessed by incubating 4 μM protein in buffer C for 10 min at selected temperatures. After the heat

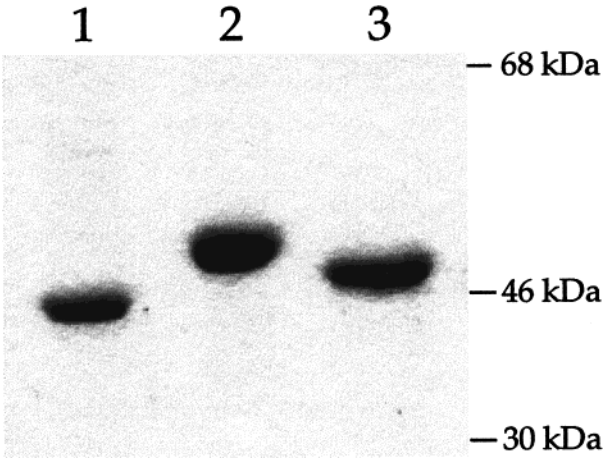

FIGURE 1: SDS−PAGE of purified *Ec*EF-Tu, *Ss*G-*Ec*MC, and *Ss*EF-1α. Two micrograms each of *Ec*EF-Tu (lane 1), *Ss*EF-1α (lane 2), or *Ss*G-*Ec*MC (lane 3) was loaded. The position after migration of the standard proteins BSA (68 kDa), ovoalbumin (46 kDa), and carbonic anhydrase (30 kDa) is shown on the right.

treatment, 25 μL aliquots were cooled on ice for 30 min and then analyzed for their [^{3}H]GDP binding ability in a final volume of 100 μL.

Melting curves of *Ss*G-*Ec*MC, *Ss*EF-1α, *Ss*G, and *Ec*EF-Tu were obtained in the temperature range of 10−99 °C at a protein concentration of 2−6 μM in buffer C using a computer-assisted Cary 1E spectrophotometer (Varian) equipped with a temperature controller. The rate of temperature increase was set at 0.2 °C/min; the difference in absorbance at 286 and 274 nm was measured every 1 °C increase, normalized between 0 and 100, and plotted versus temperature (*26*).

Three-Dimensional Modeling. The amino acid sequence of *Ss*G-*Ec*MC was submitted to the modeling program of the SwissModel server (*27*, *28*), and the crystal structure coordinates of the *Ta*EF-Tu·GppNHp·Phe-tRNA^{Phe} (*29*) ternary complex were used as a template and for superimposition (PDB file name 1TTT). The generated model was visualized by using the SwissPdbWiever program (*28*).

RESULTS

Production and Isolation of the Chimeric Elongation Factor. The chimeric elongation factor *Ss*G-*Ec*MC was expressed at high yield, and about 5 mg per liter of cell culture was obtained. The purified chimera exhibited an M_r of about 47 000 (Figure 1). Its identification was achieved by determining the sequence of the first 10 N-terminal amino acid residues which was identical to that of *Ss*EF-1α. The purified chimera was stable when stored at −20 °C in buffer B containing 50% (v/v) glycerol.

Interaction of the Chimera with Macromolecular Components Involved in Protein Synthesis. The substitution in *Ss*EF-1α of the *Ss*MC region for the corresponding *Ec*MC domain of *Ec*EF-Tu abolished in the formed chimera the property to promote poly(Phe) synthesis in either the *S. solfataricus* or *E. coli* assay system (not shown). To test if the chimera interacted with aa-tRNA, its ability to form a complex with Phe-tRNA^{Phe} was investigated. As shown in Figure 2, no complex formation was detected by gel filtration using either the chimera or the isolated *Ss*G, whereas a very weak interaction was observed for *Ss*EF-1α. The same result

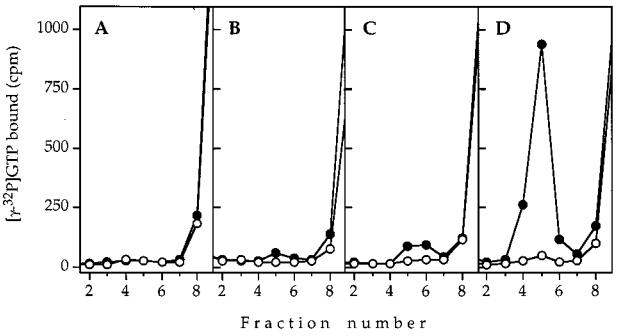

FIGURE 2: Interaction between *Ss*G-*Ec*MC, *Ss*G, *Ss*EF-1α, and *Ec*EF-Tu with *Ec*Phe-tRNA^{Phe}. The reaction mixture contained 0.2 μM *Ss*G-*Ec*MC (A), *Ss*G (B), *Ss*EF-1α (C), or *Ec*EF-Tu (D), 1 μM [γ-^{32}P]GTP (specific activity of 6200 cpm/pmol), 1 mM phosphoenolpyruvate, and 40 μg/mL pyruvate kinase in 35 μL of buffer D supplemented with 60 mM NH_4Cl. The reaction mixture was incubated for 10 min at 30 °C in the absence (white symbols) or in the presence (black symbols) of 1 μM *Ec*Phe-tRNA^{Phe} and then loaded onto a Sephadex G-25 column (0.4 cm × 15 cm), equilibrated with the above-mentioned buffer. Fractions (100 μL) were collected, and the radioactivity was measured.

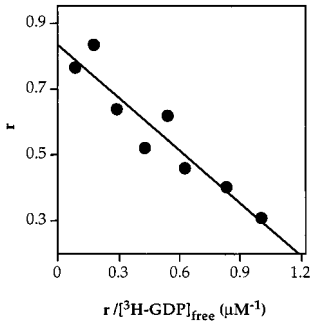

FIGURE 3: Scatchard plot for the *Ss*G-*Ec*MC·[^{3}H]GDP complex. *Ss*G-*Ec*MC (1 μM) was incubated at 60 °C in 100 μL of buffer C in the presence of 0.2−4 μM [^{3}H]GDP (specific activity of 5500 cpm/pmol). After 30 min, 90 μL aliquots were withdrawn and filtered on nitrocellulose. Each experimental point represents the average of three determinations.

Table 1: Binding of Guanine Nucleotides to *Ss*EF-1α, *Ss*G, and *Ss*G-*Ec*MC

	K_{dGDP} (μM)	K_{dGTP} (μM)	k_{-1} (min^{-1})	k_{+1} (μM^{-1} min^{-1})	ref
*Ss*G-*Ec*MC (60 °C)	0.6 ± 0.09	5.3 ± 0.3	12.7 ± 0.4	21.2 ± 2.0	this work
*Ss*EF-1α (60 °C)	1.6	35	0.14	0.09	*21*
*Ss*G (60 °C)	0.2	1.7	7.02	35.1	*13*
*Ec*EF-Tu (0 °C)	0.0009	0.5	0.014	15.6	*30*
*Ec*G (0 °C)	2.1	6.2	0.17	0.078	*30*

was obtained in other experiments in which the protection toward spontaneous deacylation of Phe-tRNA^{Phe} (from brewer's yeast or *E. coli*) by *Ss*EF-1α, *Ss*G, and the chimera in complex with GTP was tested (not shown).

Affinity of the Chimeric Elongation Factor for GDP and GTP. The chimera was able to bind GDP or GTP. The Scatchard plot shown in Figure 3 shows that GDP bound the chimera with a ratio approaching 1:1. Table 1 reports the affinity for [^{3}H]GDP and GTP of the chimera in comparison with those of *Ss*EF-1α, *Ss*G, *Ec*EF-Tu, and *Ec*G. The affinity of the chimera for both nucleotides was higher than those of *Ss*EF-1α and *Ec*G but lower than those of *Ss*G and *Ec*EF-Tu. In particular, in comparison to *Ss*EF-1α, the increase in the affinity of the chimera for GTP was much

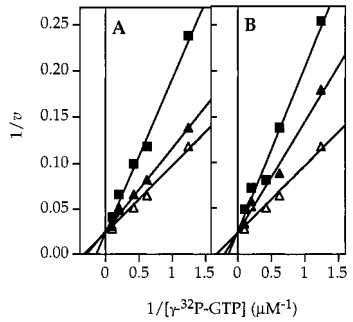

FIGURE 4: Competitive inhibition of GTPase^{Na} of *Ss*G-*Ec*MC by GDP or Gpp(NH)p. A 200 μL final volume of buffer D contained 3.6 M NaCl, 0.9 μM *Ss*G-*Ec*MC, and 0.8−10 μM [γ-^{32}P]GTP (specific activity of 3000−250 cpm/pmol) in the absence (△) or in the presence of 0.3 (▲) or 0.7 μM (■) GDP (A) or 6 (▲) or 12 μM (■) GppNHp (B). The reaction was followed kinetically at 60 °C, and the rate of release of $^{32}P_i$ was determined with 25 μL aliquots. The reaction rate (v) was expressed as moles of [γ-^{32}P]GTP hydrolyzed per minute.

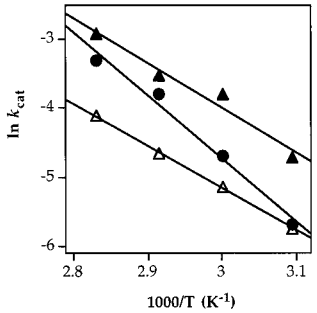

FIGURE 5: Arrhenius plot of the k_{cat} of the GTPase^{Na} of *Ss*G-*Ec*MC, *Ss*G, and *Ss*EF-1α. The k_{cat} values were determined in the temperature range of 50−80 °C as described in the legend of Figure 4. The concentration of *Ss*G-*Ec*MC (▲), *Ss*G (△), and *Ss*EF-1α (●) was 0.5 μM. Each experimental point represents the average of three determinations.

greater than that for [^{3}H]GDP. Moreover, the complex *Ss*G-*Ec*MC·[^{3}H]GDP exhibited a significant increase in both the dissociation and association rate constant. The greater increase of k_{+1} in comparison with that of k_{-1} was previously observed for *Ss*G (*13*).

The Chimeric Elongation Factor Hydrolyzes GTP. Like the intact *Ss*EF-1α, the chimeric elongation factor also elicited the intrinsic GTPase^{Na}. At 60 °C, K_m and k_{cat}, derived from the Lineweaver−Burk plot reported in Figure 4, were not significantly different from those of *Ss*EF-1α (Table 2). A more consistent increase in the catalytic efficiency of the chimeric elongation factor compared to that of *Ss*EF-1α was observed. GDP was a competitive inhibitor of GTPase^{Na} (Figure 4A) with an efficiency higher than that of Gpp(NH)p (Figure 4B); this has been reported previously for both *Ss*EF-1α and *Ss*G (*13*).

The K_m for [γ-^{32}P]GTP and the k_{cat} values of the GTPase^{Na} of the chimera, *Ss*EF-1α, and *Ss*G were also measured in the temperature interval of 30−60 °C, and they increased with increasing temperatures. Figure 5 shows the Arrhenius plots of the k_{cat} values of the GTPase^{Na}. The chimera exhibited values of the energy and entropy of activation that were lower than those of *Ss*EF-1α but similar to those of *Ss*G (Table 3).

No stimulation of the intrinsic GTPase activity of *Ss*G-*Ec*MC, *Ss*EF-1α, and *Ss*G by kirromycin at either 30 or 60 °C was observed (not shown).

The Temperature Affects the Exchange of [^{3}H]GDP for GDP or GTP on the Binary Complex SsG-EcMC·[^{3}H]GDP. The effect of temperature on the nucleotide exchange reactions was evaluated by measuring the rate constants in the interval of 0−60 °C. For both [^{3}H]GDP−GDP and [^{3}H]-GDP−GTP exchange reactions, the rate increased with increasing temperatures (Figure 6) and the corresponding Arrhenius plots were linear (Figure 7). The energetic parameters of activation for both exchange reactions were calculated at 60 °C and compared with those determined for *Ss*EF-1α and *Ss*G (Table 4). The corresponding values determined for the chimera were lower than those of *Ss*EF-1α and approaching those of *Ss*G. Such a finding was similar to that reported above for GTPase^{Na}.

Heat Stability and Thermophilicity of the Chimeric Elongation Factor. The heat inactivation profile of the [^{3}H]GDP binding ability of the chimera is reported in Figure 8A. *Ss*G-*Ec*MC was half-inactivated after exposure for 10 min at 81 °C. This value was 30 °C higher than that required to half-inactivate *Ec*EF-Tu, and 13 and 3 °C lower that those required for the half-inactivation of *Ss*EF-1α and *Ss*G, respectively.

The stabilities of *Ss*G-*Ec*MC, *Ss*EF-1α, *Ss*G, and *Ec*EF-Tu were also measured by ultraviolet-monitored thermal denaturation (*26*) of the proteins bound to GDP (Figure 8B). As it occurred for the inactivation profile of the [^{3}H]GDP binding activity shown above, the thermal stability of these proteins also increased in the order *Ec*EF-Tu, *Ss*G-*Ec*MC, *Ss*G, and *Ss*EF-1α with a denaturation midpoint of 42.4, 74.3, 86.6, and 92.2 °C, respectively. Except for *Ss*G, these values were lower compared to those determined from the inactivation curves of the [^{3}H]GDP binding (Figure 8A).

The thermophilicity of the chimera, evaluated on the basis of the GTPase^{Na}, was investigated by measuring the rate of [γ-^{32}P]GTP hydrolysis at increasing temperatures. As shown in Figure 9, the chimera exhibited a thermophilicity which at 70 °C was about 160 and 260% higher than those measured for *Ss*EF-1α and *Ss*G, respectively.

Three-Dimensional Modeling of SsG-EcMC. The superimposition of *Ss*G-*Ec*MC with the template *Ta*EF-Tu·GppNHp·Phe-tRNA^{Phe} (*29*) (Figure 10) showed that the *Ec*MC domain of the chimera was, as expected, perfectly superimposed with the *Ta*MC except for the insertion of one amino acid residue in the *Ta*M domain (P260). Vice versa, structural prediction of the *Ss*G domain showed differences which were mainly generated by the fact that the amino acid sequence of *Ss*G is longer than that of *Ta*G. In fact, the derived model of the chimeric elongation factor did not exhibit great differences in the secondary structure of *Ss*G except for its N-terminal region containing the first β-strand (V12−I17) and the first α-helix (G23−N39) of *Ta*EF-Tu. This N-terminal region was not present in *Ss*G probably because the amino acid sequence of *Ss*G contained in this region an insertion of 14 residues (*8*) which did not allow the prediction of secondary structure. Other differences included the insertion of three segments found in the chimeric model and not in *Ta*G. These were Y122−G125, V128−G130, and Y161−K164. In addition, two gaps were found in the chimeric model: one corresponding to E153 of *Ta*EF-Tu and the other corresponding to V217−K219 of *Ta*EF-Tu, in the region connecting *Ss*G to *Ec*MC.

Table 2: Catalytic and Kinetic Properties of GTPase^{Na} Supported by *Ss*EF-1α, *Ss*G, and *Ss*G-*Ec*MC and Inhibition by GDP and Gpp(NH)p (60 °C)

	k_{cat} (min^{-1})	K_m (μM)	k_{cat}/K_m (μM^{-1} min^{-1})	K_{iGDP} (μM)	$K_{iGpp(NH)p}$ (μM)	ref
*Ss*G-*Ec*MC	1.5 ± 0.2	1.7 ± 0.4	0.9 ± 0.4	1.2 ± 0.6	5.2 ± 1.2	this work
*Ss*EF-1α	0.85	2.5	0.34	1.3	8.4	*21*
*Ss*G	0.6	2.4	0.25	1.7	19.3	*13*

Table 3: Energetic Parameters of the GTPase^{Na} of *Ss*EF-1α, *Ss*G, and *Ss*G-*Ec*MC[a]

	E (kJ mol^{-1})	ΔS^* (J mol^{-1} K^{-1})	ΔG^* (kJ mol^{-1})
*Ss*G-*Ec*MC	54	−125	93
*Ss*EF-1α	76	−64	95
*Ss*G	51	−143	96

[a] The values of E were derived from the data depicted in Figure 5. ΔS^* and ΔG^* were calculated at 60 °C.

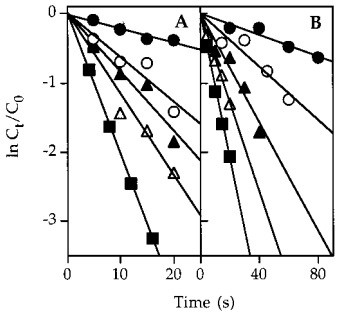

FIGURE 6: Effect of temperature on the nucleotide exchange reaction on the preformed *Ss*G-*Ec*MC·[^{3}H]GDP complex. The preformed *Ss*G-*Ec*MC·[^{3}H]GDP complex was prepared by incubating 0.5 μM *Ss*G-*Ec*MC with 6 μM [^{3}H]GDP (specific activity of 2000 cpm/pmol) for 30 min at 60 °C. The exchange reaction (200 μL) was started by adding 2 mM GDP (A) or 2 mM GTP (B) and was followed kinetically by measuring the amount of residual *Ss*G-*Ec*MC·[^{3}H]GDP in 45 μL aliquots at 0 (●), 30 (○), 40 (▲), 50 (△), and 60 °C (■).

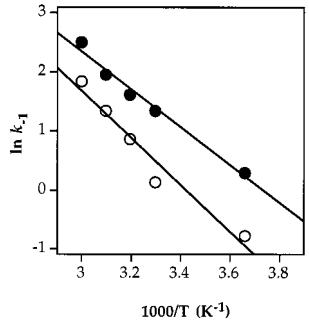

FIGURE 7: Arrhenius plot of the k_{-1} values of the nucleotide exchange reaction. The k_{-1} values for the [^{3}H]GDP−GDP (●) or [^{3}H]GDP−GTP (○) exchange reaction were derived from the data depicted in Figure 6. Each experimental point represents the average of three determinations.

DISCUSSION

In the process of protein synthesis, *Ss*EF-1α and eubacterial EF-Tu perform similar biological functions in their respective environments. EF-Tu contains structural domains, G, M, and C (*3*−*6*), which complement each other in assessing the correct folding of the whole molecule, to allow the recognition of specific nucleotides, proteins, and macromolecules (*23*, *26*). On the basis of sequence alignment, three distinct regions were identified on *Ss*EF-1α corresponding to the three structural domains of *Ec*EF-Tu (*8*, *13*). To investigate whether homologous regions could interact with their heterologous complementary domains, a chimeric elongation factor containing the archaeal thermophilic *Ss*G and the eubacterial mesophilic *Ec*MC was constructed. Its biochemical properties were compared with those of *Ss*EF-1α and *Ss*G since the latter contains the sites for the binding of guanine nucleotides and GTP hydrolysis.

A chimeric elongation factor made by the eubacterial *Ec*G and the archaeal *Ss*MC regions (*Ec*G-*Ss*MC) was also constructed and expressed in *E. coli* using the same protocol that was used for *Ss*G-*Ec*MC. Even in this case, the chimeric product accumulated in the inclusion bodies, but its isolation was fruitless because of its very low stability.

*Ss*G-*Ec*MC did not support the polymerization of phenylalanine in assay systems containing the components required for protein synthesis obtained from either *S. solfataricus* or *E. coli*. This was probably due to the fact that *Ec*MC did not recognize the archaeal macromolecules involved in this process and *Ss*G did not interact with the corresponding *E. coli* macromolecules; this last finding was confirmed by the

Table 4: Energetic Parameters of the [^{3}H]GDP−GDP and [^{3}H]GDP−GTP Exchange Reactions on the Binary Complexes Formed by [^{3}H]GDP with *Ss*EF-1α, *Ss*G, and *Ss*G-*Ec*MC[a]

binary complex	exchanger	E (kJ mol^{-1})	ΔS^* (J mol^{-1} K^{-1})	ΔG^* (kJ mol^{-1})	ref
*Ss*G-*Ec*MC·[^{3}H]GDP	GDP	27	−155	76	this work
*Ss*EF-1α·[^{3}H]GDP	GDP	63	−121	101	*13*
*Ss*G·[^{3}H]GDP	GDP	49	−123	87	*13*
*Ss*G-*Ec*MC·[^{3}H]GDP	GTP	33	−142	77	this work
*Ss*EF-1α·[^{3}H]GDP	GTP	76	−80	100	*13*
*Ss*G·[^{3}H]GDP	GTP	40	−154	88	*13*

[a] The values of E were determined in the temperature range of 0−60 °C. ΔS^* and ΔG^* were calculated at 60°C.

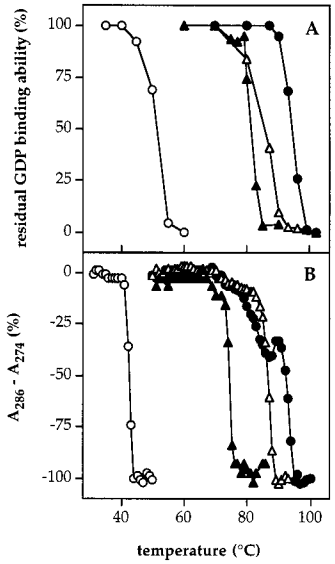

FIGURE 8: Heat stability of *Ec*EF-Tu, *Ss*G-*Ec*MC, *Ss*G, and *Ss*EF-1α. (A) Residual [^{3}H]GDP binding ability and (B) melting curves of *Ss*EF-1α (●), *Ss*G-*Ec*MC (▲), *Ss*G (△), and *Ec*EF-Tu (○). Each experimental point represents the average of three determinations.

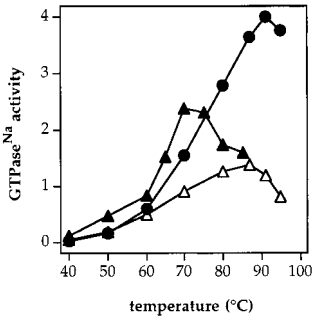

FIGURE 9: Thermophilicity of *Ss*EF-1α, *Ss*G, and *Ss*G-*Ec*MC. The GTPase^{Na} activity was assayed as described in Materials and Methods in a final volume of 200 μL and reported as moles of [γ-^{32}P]GTP hydrolyzed per minute per mole of protein: *Ss*EF-1α (●), *Ss*G-*Ec*MC (▲), and *Ss*G (△).

FIGURE 10: 3D model of *Ss*G-*Ec*MC superimposed with the 3D structure of *Ta*EF-Tu·GppNHp in complex with Phe-tRNA^{Phe}. *Ss*G-*Ec*MC is black and *Ta*EF-Tu blue. A represents the N-terminal region missing in the *Ss*G-*Ec*MC model. B and C represent insertions (red) and D−F gaps (green) in the chimeric model. See the text for details.

fact that *Ss*G-*Ec*MC did not form a complex with *Ec*Phe-tRNA^{Phe} and GTP (Figure 2).

Despite its inability to sustain poly(Phe) synthesis, the chimeric elongation factor retained some important properties of *Ss*EF-1α, such as the ability to bind guanine nucleotides and to hydrolyze GTP. In fact, it bound either GDP or GTP with an affinity that was higher than that exhibited by *Ss*EF-1α but significantly lower than that exhibited by *Ec*EF-Tu (Table 1). Since the removal of *Ss*MC from *Ss*EF-1α increased greatly the affinity for guanine nucleotides and the insertion of *Ec*MC restored partially the values of K_{dGDP} and K_{dGTP}, a weak interaction between *Ss*G and *Ec*MC can be cited, at least concerning the affinity for nucleotides. The increased affinity of the chimera for GDP and GTP was due to the association rate constant which increased much more compared to the dissociation rate constant (Table 1). The increased affinity of the chimera for the guanine nucleotides can also be explained with the energetic data reported in Table 4. In fact, for both the [^{3}H]GDP−GDP and [^{3}H]GDP−GTP exchange reactions, the process was favored by a significant decrease in the activation energy with respect to *Ss*EF-1α and *Ss*G as well. The free energy of activation exhibited a moderate decrease, accompanied by a decrease in the activation entropy that was greater when the exchanger was GTP. This last finding suggested that the binding of GTP generated a transition state with a more compact structure of the chimeric elongation factor compared to that occurring upon the binding of GDP. This might be in agreement with the results of crystallographic data showing that *T. thermophilus* EF-Tu·GTP has a more compact molecular organization than *Ec*EF-Tu·GDP (*4*−*7*).

The catalytic efficiency of GTPase^{Na} of the chimeric elongation factor was higher than that of either *Ss*EF-1α or *Ss*G (Table 2). The inhibition constants for GDP and Gpp(NH)p were comparable to those of *Ss*EF-1α, thus suggesting that in the presence of high salt concentrations the *Ec*MC domain of the chimeric elongation factor did not alter the level of exposure of the binding site for guanine nucleotides on *Ss*G. The comparison between the K_d values reported in Table 1 with the K_i values reported in Table 2 showed that 3.6 M NaCl reduced the affinity of the chimera for GDP; this suggested that the salt made the guanine nucleotide binding site less accessible to GDP. The energetic values reported in Table 3 might explain the above results. In fact, although the value of the activation energy of GTPase^{Na} of *Ss*G-*Ec*MC was lower than that of both *Ss*EF-1α and *Ss*G, the free energy of activation was almost the same for all three systems.

Since about half of the *Ss*G-*Ec*MC primary structure was of mesophilic origin, it should be expected that the temperature for half-inactivation of the chimeric elongation factor was lower than that observed (Figure 8A). Despite that, the chimera was much more stable than *Ec*EF-Tu. This behavior could be explained by the fact that in the chimeric elongation factor, *Ec*MC did not provoke a substantial reduction in the average amino acid hydrophobicity of the whole molecule. In fact, as previously reported, the average hydrophobicity of proteins increases with the increase of the optimum temperature at which they are still active (*31*, *32*). In the case presented here, the average amino acid hydrophobicities calculated for *Ss*G-*Ec*MC, *Ss*EF-1α, and *Ec*EF-Tu were 4.8, 4.9, and 4.6 kJ/amino acid, respectively, thus explaining why the stability of the chimera was closer to that of *Ss*EF-1α than to that of *Ec*EF-Tu. To exclude the possibility that the stability of the chimeric factor was correlated mainly with the stability of the *Ss*G, thermal denaturation profiles of *Ec*EF-Tu, *Ss*G-*Ec*MC, SsG, and *Ss*EF-1α were obtained. The pattern of the melting curves (Figure 8B) was similar to that obtained from the measurements of the heat inactivation (Figure 8A) except for the melting curve of *Ss*EF-1α which appeared to be caused by different structural events. When the naturally occurring form of *Ss*EF-1α was tested instead, the denaturation profile was like that usually observed for the melting curves (not shown). The temperatures for half-inactivation (Figure 8A) were higher than the temperatures for half-denaturation derived from the melting curves (Figure 8B). Such a difference might be due to the fact that the proteins remained functioning even if a moderate denaturation occurred. In addition, since during the thermal denaturation the proteins were exposed to sequentially higher

temperatures, an additive effect of the exposure to higher temperatures cannot be excluded.

The replacement of *Ss*MC for *Ec*MC yielded a lower denaturation midpoint temperature (from 92.2 °C for *Ss*EF-1α to 74.3 °C for *Ss*G-*Ec*MC), thus indicanting that the interaction of *Ec*MC with *Ss*G destabilizes somehow the entire chimeric molecule.

The *Ec*MC domain contributed to the increase in the thermophilicity of the chimera in comparison to those of *Ss*EF-1α and *Ss*G (Figure 9). In fact, up to 70 °C the chimera was more active than *Ss*EF-1α. Above 70 °C, the chimera began to inactivate.

The chimeric elongation factor exhibited a [^{3}H]GDP−GTP exchange rate which was 2 orders of magnitude higher than that of *Ss*EF-1α, in agreement with the lower activation energy values reported in Table 4. In a previous work from this laboratory, it was shown that the nucleotide exchange factor *Ss*EF-1*β* did not have any stimulatory effect on the [^{3}H]GDP−GTP exchange on *Ss*G·[^{3}H]GDP (*13*). A similar effect was also observed for the chimera, since even at 0 °C the exchange reaction proceeded too fast to allow the detection of any stimulatory effect by *Ss*EF-1*β* (data not shown).

To explain the inability of the chimeric elongation factor to promote poly(Phe) synthesis, to interact with aa-tRNA, and to bind kirromycin, a model was constructed using as template the 3D structure of the ternary *Ta*EF-Tu·GppNHp·Phe-tRNA^{Phe} complex (*29*) (Figure 10). The amino acid residues required for the binding of aa-tRNA are almost all conserved, an exception being made for a few residues of the effector loop (K52−N64 in *Ta*EF-Tu). In particular, residues K52, A53, and P54 of *Ta*EF-Tu are replaced in the chimeric elongation factor with R61, L62, and K63, respectively. However, these substitutions did not explain the lack of interaction between the chimeric elongation factor and Phe-tRNA^{Phe} (Figure 2), it having been reported that the binding of aa-tRNA to *Ta*EF-Tu occurred even if the entire effector region was deleted (*33*, *34*).

The amino acid residues involved in the binding of the antibiotic kirromycin, which in domain G of *Ta*EF-Tu are L120, Q124, and Y160, in the G domain of the chimeric factor corresponded to I137, T141, and Y180, respectively. Since in *Ta*EF-Tu the binding site for the antibiotic is supposed to be at the interface of domains G and C and to involve most likely Q124 (*35*), the lack of interaction of *Ss*G-*Ec*MC with kirromycin might be ascribed to the presence of T141 in this position, in agreement with the result previously reported in which the mutation Q124K in *Ec*EF-Tu makes the elongation factor resistant to kirromycin (*35*).

In conclusion, a more appropriate evaluation of all the points considered above can be carried out after the 3D structure of *Ss*EF-1α is determined. Furthermore, the results reported in this work indicate that homologous domains of proteins with a distant evolutionary pathway are not interchangeable, since correct interactions between structural domains may be critical for maintaining their biological functions.

ACKNOWLEDGMENT

We are grateful to A. Parmeggiani (Ecole Polytechnique, Palaiseau, France) for supplying the pGEX-2T plasmid containing the *E. coli tuf*A gene and for assessing the poly(Phe) synthesis of the chimeric elongation factor in the *E. coli* assay system. The skillful technical assistance of A. Fiengo is gratefully acknowledged.

REFERENCES

1. Baldauf, S. L., Palmer, J. D., and Ford Doolittle, W. (1996) *Proc. Natl. Acad. Sci. U.S.A. 93*, 7749−7754.
2. Dever, T. E., Glynias, M. J., and Merrick, W. C. (1987) *Proc. Natl. Acad. Sci. U.S.A. 84*, 1814−1818.
3. Kjeldgaard, M., and Nyborg, J. (1992) *J. Mol. Biol. 223*, 721−742.
4. Song, H., Parson, M. R., Rowsell, S., Leonard, G., and Phillips, S. E. (1999) *J. Mol. Biol. 285*, 1245−1256.
5. Berchtold, H., Reshetnikova, L., Reiser, C. O. A., Schirmer, N. K., Sprinzl, M., and Hilgenfield, R. (1993) *Nature 365*, 126−132.
6. Kjeldgaard, M., Nissen, P., Thirup, S., and Nyborg, J. (1993) *Curr. Biol. 1*, 35−50.
7. Sprinzl, M. (1994) *Trends Biochem. Sci. 19*, 245−250.
8. Arcari, P., Gallo, M., Ianniciello, G., Dello Russo, A., and Bocchini, V. (1994) *Biochim. Biophys. Acta 1217*, 333−337.
9. Zagari, A., Sica, F., Scarano, G., Vitagliano, L., and Bocchini, V. (1994) *J. Mol. Biol. 242*, 175−177.
10. Masullo, M., Raimo, G., and Bocchini, V. (1993) *Biochim. Biophys. Acta 1161*, 35−39.
11. Masullo, M., Raimo, G., Parente, A., Gambacorta, A., De Rosa, M., and Bocchini, V. (1991) *Eur. J. Biochem. 199*, 529−537.
12. Masullo, M., De Vendittis, E., and Bocchini, V. (1994) *J. Biol. Chem. 269*, 20376−20379.
13. Masullo, M., Ianniciello, G., Arcari, P., and Bocchini, V. (1997) *Eur. J. Biochem. 243*, 468−473.
14. Motoki, K., Kitajima, Y., and Hori, K. (1993) *J. Biol. Chem. 268*, 1677−1683.
15. Terashima, M., Kawai, M., Kumagai, M. H., Rodriguez, R. L., and Katoh, S. (1996) *Appl. Microbiol. Biotechnol. 45*, 607−611.
16. Satoh, T., Takahashi, Y., Oshida, N., Shimizu, A., Shinoda, H., Watanabe, M., and Samajima, T. (1999) *Biochemistry 38*, 1531−1536.
17. Ianniciello, G., Gallo, M., Arcari, P., and Bocchini, V. (1994) *Biochem. Mol. Biol. Int. 33*, 927−937.
18. Maniatis, T., Fritsch, E. F., and Sambrook, J. (1982) *Molecular Cloning. A Laboratory Manual*, Cold Spring Harbor Laboratory Press, Cold Spring Harbor, NY.
19. Smith, D. B., and Johnson, K. S. (1988) *Gene 67*, 31−40.
20. Deng, W. P., and Nickoloff, J. A. (1992) *Anal. Biochem. 200*, 81−88.
21. Ianniciello, G., Masullo, M., Gallo, M., Arcari, P., and Bocchini, V. (1996) *Biotechnol. Appl. Biochem. 23*, 41−45.
22. Studier, F. W., Rosemberg, A. H., Dunn, J. J., and Dubendorff, J. W. (1990) *Methods Enzymol. 185*, 60−89.
23. Cetin, R., Anborgh, P. H., Cool, R. H., and Parmeggiani, A. (1998) *Biochemistry 37*, 486−495.
24. Fasano, O., Bruns, W., Crechet, J. B., Sander, G., and Parmeggiani, A. (1978) *Eur. J. Biochem. 89*, 557−565.
25. Raimo, G., Masullo, M., Savino, G., Scarano, G., Ianniciello, G., Parente, A., and Bocchini, V. (1996) *Biochim. Biophys. Acta 1293*, 106−112.
26. Nock, S., Grillenbeck, N., Ahmadian, M. R., Ribeiro, S., Kreutzer, R., and Sprinzl, M. (1995) *Eur. J. Biochem. 234*, 132−139.
27. Peitsch, M. C. (1996) *Biochem. Soc. Trans. 24*, 274−279.
28. Guex, N., and Peitsch, M. C. (1997) *Electrophoresis 18*, 2714−2723.
29. Nissen, P., Kjeldgaard, M., Thirup, S., Polekhina, G., Reshetnikova, L., Clark, B. F. C., and Nyborg, J. (1995) *Science 270*, 1464−1472.

30. Jensen, M., Cool, R. H., Mortensen, K. K., Clark, B. F. C., and Parmeggiani, A. (1989) *Eur. J. Biochem. 183*, 247−255.
31. De Vendittis, E., and Bocchini, V. (1996) *Gene 176*, 27−33.
32. Dello Russo, A., Rullo, R., Nitti, G., Masullo, M., and Bocchini, V. (1997) *Biochim. Biophys. Acta 1343*, 23−30.
33. Nissen, P., Kjeldgaard, M., Thirup, S., Clark, B. F. C., and Nyborg, J. (1996) *Biochimie 78*, 921−933.
34. Ott, G., Jonak, J., Abrahams, I. P., and Sprinzl, M. (1990) *Nucleic Acids Res. 18*, 437−441
35. Mester, J. R., Zeef, L. A. H., Hilgenfeld, R., de Graaf, J. M., Kraal, B., and Bosch, L. (1994) *EMBO J. 13*, 4877−4885.

BI990418D